Sensors and Materials, Vol. 34, No. 11 (2022) 4209–4222
MYU Tokyo

S & M 3106

Investigation of Drift in Polyurethane Matrices for Salivary Nitrate Ion-selective Field-effect Transistors

Shuto Osaki,[1,2*] Kenichi Kitamura,[1,3] Takuya Kintoki,[1,4]
Takayo Moriuchi-Kawakami,[4] and Shin-ichi Wakida[1]

[1]AIST–Osaka University Advanced Photonics and Biosensing Open Innovation Laboratory, AIST, 2-1 Yamadaoka 2, Suita, Osaka 565-0871, Japan
[2]Osaka University, Graduate School of Engineering, 2-1 Yamadaoka 2, Suita, Osaka 565-0871, Japan
[3]Maritime Technology Department, National Institute of Technology, Toba College, 1-1 Ikegami-cho, Toba, Mie 517-8501, Japan
[4]Department of Applied Chemistry, Graduate School of Engineering, Osaka Institute of Technology, 16-1 Oomiya 5, Asahi-ku, Osaka 535-8585, Japan

(Received September 16, 2022; accepted November 4, 2022)

Keywords: ion-selective membrane, ISFETs, polyurethane, salivary nitrate, stress monitoring

We systematically investigated the drift of ion-selective field-effect transistors (ISFETs) using a series of polyurethanes as a polymer matrix. Drift is one of the shortcomings of ISFETs that adopt a polymeric ion-selective membrane. The drift is caused by the pH change in the aqueous layer between the ion-selective membrane and the pH-sensitive gate of the ISFET. We previously reported NO_3^--ISFETs with a novel polyurethane P7281-PU, which give specific stable values. This polyurethane showed less drift than conventional polyvinyl chloride. We considered that the urethane bonds in the ion-selective membrane might capture the diffused H^+ or OH^- ions that induce the drift. In this study, we investigate a polyurethane composed of an ion-selective membrane and consider how the condition and performance of the ion-selective membrane affect the drift. We selected eight types of polyurethane with almost the same composition as P7281-PU for comparison. We confirmed a narrower variation range of 4.5 mV/h from ISFETs with polyurethane P7293-PU than those of 33.7 mV/h from PVC and 5.0 mV/h from P7281-PU through drift tests using artificial saliva. From the tests, we also confirmed that the drift prevention effect might be caused by the ion-trapping sites generated with the hydrolysis of the urethane bonds.

1. Introduction

Mental stress measurement is an important issue, because mental stress is associated with various diseases and physical disorders. The diathesis-stress model may provide evidence for a disease pathogenesis of depression. According to this model, depression is associated with genetic vulnerability of the central nervous system and external environmental stress.[1–4] Therefore, we aim to detect mental workload in point-of-care testing (POCT) and create a

*Corresponding author: e-mail: osaki@ap.eng.osaka-u.ac.jp
https://doi.org/10.18494/SAM4105

ISSN 0914-4935
https://myukk.org/

portable device for anyone to easily obtain diagnosis results of stress measurement. We consider that the portable device can convert stress into numerical values to clarify the stress state and that this device will contribute to increasing our quality of life.

Conventionally, mental stress is evaluated by subjective psychological tests such as the Profile of Mood States (POMS) and Cornell Medical Index (CMI).[5] We aim to establish an objective method for quantitative mental workload evaluation. Regarding objective biochemical methods, researchers have focused on the stress markers in body fluids such as serum, urine, and saliva.[6–8] In particular, blood contains the typical stress markers of adrenaline and noradrenalin,[9,10] which are expected to be useful stress markers. However, blood cannot be collected non-invasively. In contrast, blood-borne saliva can be collected non-invasively. Therefore, we focused on saliva as an effective body fluid that includes various stress markers such as blood to measure acute stress.[11] Finally, we selected the concentration of NO_3^- in saliva as an indicator of stress, a higher NO_3^- concentration indicating higher stress.

One of the nitric oxide (NO) metabolites in blood is NO_3^-, and salivary NO_3^- is secreted through the salivary gland from blood.[12] NO is an endothelium-derived relaxing factor (EDRF) produced in response to the vascular tone by the autonomic nervous system.[13] In brief, salivary NO_3^- is controlled by the autonomic nervous system and is expected to have a more rapid response to mental workload than other stress markers in the body.[14] On the other hand, other salivary stress markers such as cortisol, immunoglobulin A, chromogranin A, and α-amylase are not suitable for on-site stress monitoring; these stress markers are mainly measured by enzyme-linked immunosorbent assay (ELISA), which requires a long time to obtain results.[15–18]

As measurement devices, we adopted NO_3^- ion-selective field-effect transistors (NO_3^--ISFETs), which indicate the NO_3^- concentration in a target liquid (here saliva). ISFETs require only 1 ml of saliva without post-measurement analysis to obtain values. In fact, NO_3^--ISFETs can obtain NO_3^- concentration values from on-site analysis within 10 s. On the other hand, NO_3^--ISFETs have the shortcoming of drift in salivary measurement, where their response values to saliva fluctuate owing to some phenomena. Owing to the major problem of drift, no researchers have shown interest in the measurement of salivary ions using ISFETs; other drift studies were performed without using saliva and did not require long-time measurement. From our preceding studies to evaluate mental workload with NO_3^--ISFETs,[19,20] we realize that conventional ISFETs require calibration every after measurement to show accurate values. We aim to develop new NO_3^--ISFETs without drift for long-term saliva immersion. To prevent drift, we have focused on the polymer component of a specific membrane on NO_3^--ISFETs called an ion-selective membrane (ISM).

Regarding other drift prevention studies related to ISFETs, Fogt *et al.* reported that drift is caused by a pH change in the aqueous layer between the ISM and the pH-sensitive gate of ISFETs.[21] Patrick *et al.* reported that drift involves H^+ ions (generated by CO_2^- gas + H_2O) and an organic acid, and H^+ ions approach the aqueous layer between the ISM and the gate interface through the ISM.[22] We assume that this drift may also occur in our study, because saliva includes HCO^-.

On the other hand, Abramova *et al.* considered that drift is caused by the adsorption of blood protein on the ISM surface.[23] ISFETs based on conventional polyvinyl chloride (PVC) show drift in the measurement of blood plasma. Saliva contains several proteins and its pH is

approximately 7.[24] We consider that salivary proteins are absorbed onto the membrane, and H^+ or OH^- are diffused in the membrane and change the pH in the aqueous layer between the gate of the ISFET and the membrane.

Therefore, we assume that salivary nitrate derived from blood will show an unstable response to blood plasma. To reduce the drift of ISFETs, previous studies involved inserting an inner layer between the ISM and the gate interface, for example, a pHEMA-gel saturated buffer, Ag/AgCl, or a H^+-selective membrane or parylene.[22,25–27] Other studies reported that the formation of an aqueous layer was prevented by improving the adhesion between the ISM and the gate interface.[28]

Our previously hypothesized drift prevention effect of the P7281-PU matrix membrane is shown in Fig. 1. We previously reported on drift and the hypothesis that the ISM on ISFETs composed of P7281-PU prevents drift.[29] ISFETs based on the reported polyurethane (P7281-PU) showed a more stable response than those based on conventional PVC and other polyurethane-based matrices (Pellethane® and KP-13).

In this study, we investigated the hypothesized drift prevention effect of P7281-PU in our previous paper. We prepared eight types of polyurethane, P7281-PU and seven other polyurethanes with the same backbone as P7281-PU but different molecular weights. We focused on the physical characteristic of the polyurethane matrix because we could not describe the drift with our previous hypothesis. We found that when a hydrophilic polyurethane matrix was employed, drift occurred as a result of the physical cracking of the membrane structure by the drift-tested solution. The surface of each membrane was observed using an optical microscope before and after the drift. We proposed our improved drift hypothesis based on the hydrolysis of urethane bonds and the miscibility between the liquid membrane and the polymers.

2. Materials and Methods

2.1 Materials

PVC (n = 1020) was purchased from Kishida Chemical (Osaka, Japan). A series of P72XX-PU polymers (P7276-PU, P7277-PU, P7283-PU, P7286-PU, P7287-PU, P7290-PU, P7293-PU,

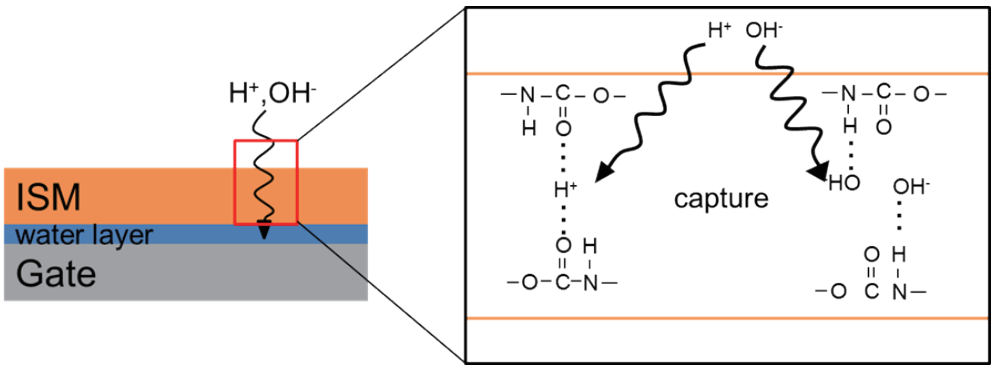

Fig. 1. (Color) Hypothesized urethane bond capture of H^+ and OH^- by hydrogen bonds (in whole saliva) from our previous report.[29]

and P7281-PU) were purchased from Polymer Source (Dorval, QC, Canada). The P72XX-PU series were synthesized from 4,4'-methylenebis(phenyl isocyanate) (MDI), poly(propylene oxide) (PPO), and Bisphenol A ethoxylate (BPAEO). We chose this series because P7281-PU and the other polyurethanes with the same backbone structure (Fig. 2) have different molecular weights. The physical properties and chemical structure of the P72XX-PU series were obtained from a data sheet; the structure is shown in Fig. 2 and the molecular weights of the series are summarized in Table 1. P7281-PU has a much higher molecular weight than the others. These materials were used for the membrane matrix. Bis(bathocuproin)-copper (I) nitrate ($[Cu(bcp)_2]NO_3$) was synthesized as described in Ref. 8 and used for the ionophore. 2-nitrophenyl dodecyl ether (NPDDE) was purchased from Fujifilm Wako Pure Chemical (Osaka, Japan) and used to enhance hydrophobicity and the adhesiveness to an ISM.[30] Tetrahydrofuran (THF), KNO_3, NaCl, KCl, KH_2PO_4, urea, Na_2SO_4, NH_4Cl, $CaCl_2{\cdot}2H_2O$, $NaHCO_3$, KI, KSCN, and $NaNO_2$ were purchased from Wako Pure Chemical (Osaka, Japan). THF was used as a volatile solvent to dissolve the nitrate ionophore, plasticizer, and membrane matrix. These chemicals were analytical grade, except for $NaNO_2$, which was volumetric analysis grade. All standard solutions and artificial saliva were prepared with Milli-Q water (18.2 M·Ωcm).

2.2 Preparation of NO_3^--ISFETs

The nitrate-selective membrane was prepared by mixing 5 wt% of the nitrate ionophore ($[Cu(bcp)_2]NO_3$), 65 wt% of the plasticizer (NPDDE), and 30 wt% of the membrane matrix. Then, they were completely dissolved in the THF solution at room temperature. NO_3^--ISFETs were prepared by casting the THF solution above the gate of the specially ordered pH-ISFETs

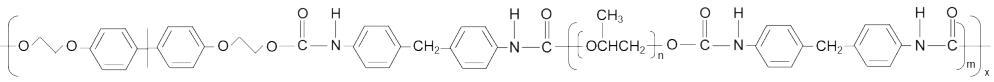

Fig. 2. (Color online) Structure of P72XX-PU series.

Table 1
Molecular weight and monomer rate of each polyurethane.

Polyurethane	MDI	PPO	BPAEO	Mn	Mw
P7281-PU	1.35	0.82	0.41	55200	259400
P7276-PU	1.35	1.18	0.49	14100	25400
P7277-PU	1.8	0.91	0.79	22400	49700
P7283-PU	1.35	0.93	0.38	5700	10800
P7286-PU	1.8	0.74	0.56	18500	40700
P7287-PU	1.8	0.91	0.79	10600	28400
P7290-PU	1.35	1.47	0.25	11400	18200
P7293-PU	1.8	0.7	0.54	10600	16900

(S2K922: ISFETCOM Co., Ltd.) using a pipette tip (Fig. 3). The gate of ISFETs consists of a H^+-selective metal oxide, for example, Ta_2O_5, SiO_2, or S_3N_4. In this study, we used the Ta_2O_5 gate part on the ISFETs, which shows a stable response for pH sensing over hundreds of hours.[31] We also used a single-junction reference electrode (R2K712: ISFETCOM Co., Ltd.), which shows a stable response during tens of hours of pH measurement.[32] The reference electrode consisted of a Ag/AgCl electrode and saturated KCl solution to connect with the sample via a ceramic liquid junction.

The casting process was repeated several times. The gate of the ISFETs was filled with THF solution. The THF solution on the gate evaporated in the clean space (Pure space 01; AS ONE; Osaka, Japan). The nitrate-selective membrane had a thickness of ca. 0.2 mm and a flat surface. The NO_3^--ISFETs were completely dried over 8 h. The ISMs of the NO_3^--ISFETs were immersed in a conditioning solution of 10^{-3} M KNO_3 for about 3 h.

2.3 Evaluation of calibration curves and selectivity coefficients for NO_3^--ISFETs

We systematically studied the sensitivity and selectivity for the ISMs based on PVC, KP-13, P7281-PU, P7276-PU, P7277-PU, P7283-PU, P7286-PU, P7287-PU, P7290-PU, and P7293-PU. Calibration curves and selectivity coefficients of the NO_3^--ISFETs were evaluated using the Nikolsky–Eisenman equation [Eq. (1)]. Here, E is the gate potential of the NO_3^--ISFET, $E0$ is the standard potential of the NO_3^--ISFET, Z_i and Z_j are the changes in the concentrations of the target ion i (NO_3^-) and the interfering ion j, and coefficients a_i and a_j are their activities, respectively.

$$E = E_0 + 2.303RT / Z_i F \ln\left(a_i + K_{ij}^{pot} \left(a_j \right)^{Z_i / Z_j} \right) \tag{1}$$

R, T, and F have their conventional meanings. According to the theoretical response at 25 °C, the slope sensitivity of the NO_3^--ISFET is the change in the activity (a_i), which is −59.16 mV per decade. The coefficients a_i were calculated from the Debye–Hückel equation based on simple ionic strength theory. K_{ij}^{pot} is the selectivity coefficient of the NO_3^--ISFET having interfering

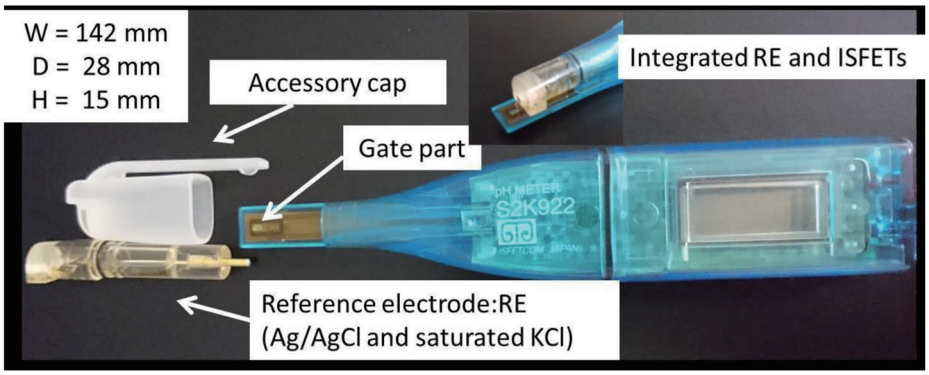

Fig. 3. (Color online) pH-sensitive pH-ISFETs and accessory cap.

ion *j* and is evaluated by the mixed-solution method, which gives a reliable selectivity parameter. The potential responses were measured for KNO_3 solution, including five types of general interfering ions: 5.0×10^{-1} mol/L (M) NaCl, 5.0×10^{-1} M Na_2SO_4, 5.0×10^{-2} M $NaNO_2$, 5.0×10^{-5} M KI, and 5.0×10^{-5} M KSCN.

2.4 Evaluation of initial drift for NO_3^--ISFETs

We carried out drift tests to determine the stability of the NO_3^--ISFETs along with their sensitivity and selectivity. The initial drift was evaluated by examining the potential value of the NO_3^--ISFETs immersed in each solution for about 8 h. Three different solutions, 1.0×10^{-3} M KNO_3 (standard solution), mucin solution, and artificial saliva, were prepared for the drift tests. The mucin solution was prepared by adding 0.5 wt% mucin to the standard solution. Artificial saliva contains salivary inorganic salts and urea and includes 2.15 mM NaCl, 12.9 mM KCl, 4.81 mM KH_2PO_4, 0.33 mM urea, 2.37 mM Na_2SO_4, 3.33 mM NH_4Cl, 1.55 mM $CaCl_2{\cdot}2H_2O$, 7.51 mM $NaHCO_3$, and 1.0 mM KNO_3. We changed the ISM in every drift test. The drift test was performed several times for each type of sample.

2.5 Observation of ISM before and after drift

We observed eight types of polyurethane membranes to elucidate the hypothesized drift prevention effect of P7281-PU. The surfaces of the ISMs were observed using an optical microscope (KH-8700; HIROX Co., Ltd., Tokyo, Japan) before and after drift measurement in KNO_3 standard solution. After the drift measurement, the ISM on the gate was washed with Milli-Q water. Then, the membranes were observed using an optical microscope. Figure 4 shows one of the ISFETs, where we observed optical images from the surface of its gate covered by the ISM.

3. Results and Discussion

3.1 Calibration curves and selectivity coefficients

We systematically studied the sensitivity and selectivity of the ISFETs based on PVC, P7276-PU, P7277-PU, P7283-PU, P7286-PU, P7287-PU, P7290-PU, P7293-PU, and P7281-PU. The calibration curves of the NO_3^--ISFETs are shown in Fig. 5, where the x-axis is the logarithm of the nitrate activity and the y-axis is the potential difference. NO_3^--ISFETs based on PVC, P7276-PU, P7277-PU, P7286-PU, P7293-PU, and P7281-PU showed approximately the same linear response range from 10^{-5} to 10^{-1} mol/L (M)[29] and had close to the theoretical slope response of 59.2 mV/decade at 25 °C according to the Nernst equation. The concentration range of salivary nitrate is approximately 10^{-4} to 10^{-3} M.[33] Therefore, these ISFETs may be suitable for the determination of salivary nitrate. On the other hand, the NO_3^--ISFETs based on P7283-PU, P7287-PU, and P7290-PU did not show reproducibility due to the unstable sensor responses. Therefore, we did not perform experiments on the unstable NO_3^--ISFETs to measure their selectivity coefficients and drift. Table 2 shows the slopes in the linear response range.

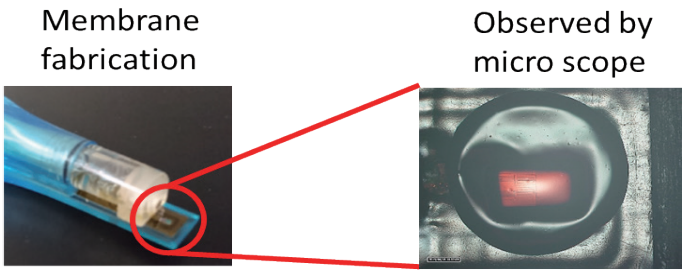

Fig. 4. (Color online) Details of ISFET and optical image of ISM.

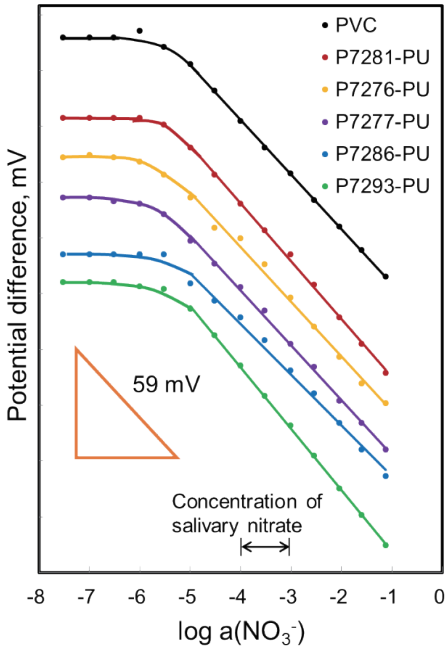

Fig. 5. (Color online) Calibration curves.

Table 2
Slope of the calibration curves (n = 3).

Polymer matrix	Slope of the linear response range (mV/decade)
PVC	61.1 ± 2.3
P7281-PU	61.5 ± 0.70
P7276-PU	64.1 ± 5.5
P7277-PU	51.1 ± 4.0
P7286-PU	57.2 ± 10.8
P7293-PU	65.7 ± 0.70

The selectivity coefficients Kij^{pot} of the NO_3^--ISFETs were calculated using the Nikolsky–Eisenman equation and measured by the mixed-solution method for five typical interfering anions (Cl^-, SO_4^{2-}, NO_2^-, I^-, SCN^-). Their results are summarized in Table 3 and follow the well-known Hofmeister series. The NO_3^--ISFETs based on the P72XX-PU series exhibited sensitivity and selectivity, similarly to the ISFETs based on conventional PVC and P7281-PU.[29]

Table 3
Selectivity coefficients, $\log K^{pot}_{NO_3^-,j}$.

Polymer matrix	Selectivity coefficients, $\log K^{pot}_{NO_3^-,j}$.				
	I	SCN	NO_2	Cl	SO_4
PVC	0.80	1.05	−1.53	−2.50	−4.15
P7281-PU	0.76	0.92	−1.56	−2.52	−4.21
P7276-PU	0.80	0.85	−1.51	−2.30	−4.12
P7277-PU	0.86	0.96	−1.50	−2.45	−4.18
P7286-PU	0.74	1.06	−1.38	−2.27	−4.34
P7293-PU	0.84	1.11	−1.42	−2.23	−4.28

Therefore, the potential of NO_3^--ISFETs is determined by their nitrate ionophore ($[Cu(bcp)_2]NO_3$) and plasticizer (NPDDE) but not their membrane matrix. The non-reproducible response of the ISFETs based on P7283-PU, P7287-PU, and P7290-PU may have been caused by miscibility among the ionophore, plasticizer, and polymer. These phenomena were not observed for our previous polymer of P7281-PU.[29]

3.2 Evaluation of initial drift

Figure 5 shows the drift characteristics of the NO_3^--ISFETs based on PVC, P7281-PU, and the P72XX series under various conditions. The x-axis is the logarithm of time, and the y-axis is the potential difference. The results of drift are arranged with different starting points to understand the potential fluctuation. Figure 6 shows the drift with NO_3^--ISFETs based on the P72XX-PU series, and the potential indicator was inserted for easy comparison of the membranes from each potential difference.

We observed that the drift characteristics were almost the same for the several types of samples. In the standard solution, all NO_3^--ISFETs showed a comparatively stable response [see Fig. 6(a)] excluding the ones based on P7276-PU. The ISFETs based on P7276-PU did not show a stable response in all solutions. In mucin solution, the ISFETs based on PVC showed drift, but the other ISFETs based on the P72XX-PU series showed a comparatively stable response [see Fig. 6(b)]. The ISFETs based on P7293-PU showed the most stable response in the P72XX-PU series. Therefore, mucin, one of the salivary proteins, has less influence on the drift for the NO_3^--ISFETs based on PVC than for the NO_3^--ISFETs based on the P72XX-PU series.

In sodium bicarbonate solution, the NO_3^--ISFETs based on P7281-PU and P7293-PU showed a similar stable response [Fig. 6(c)]. On the other hand, the NO_3^--ISFETs based on PVC showed drift, and the NO_3^--ISFETs based on P7276-PU, P7277-PU, P7286-PU, P7293-PU showed slightly less drift. In artificial saliva, all ISFETs except for those based on P7281-PU and P7293-PU showed drift [Fig. 6(d)]. Figures 6(c) and 6(d) suggest that the drift may be caused by bicarbonate ions, because artificial saliva includes sodium bicarbonate. For the drift in artificial saliva, the variation range was calculated to be 33.7 ± 2.8 mV/h for PVC, 5.0 ± 0.63 mV/h for P7281-PU, 4.5 ± 2.3 mV/h for P7293-PU, 8.5 ± 2.9 mV/h for P7276-PU, and 6.4 ± 0.62 mV/h for P7277-PU (n = 3). The ISFETs based on P7281-PU and P7293-PU showed the most stable drift prevention effect of the membrane matrix.

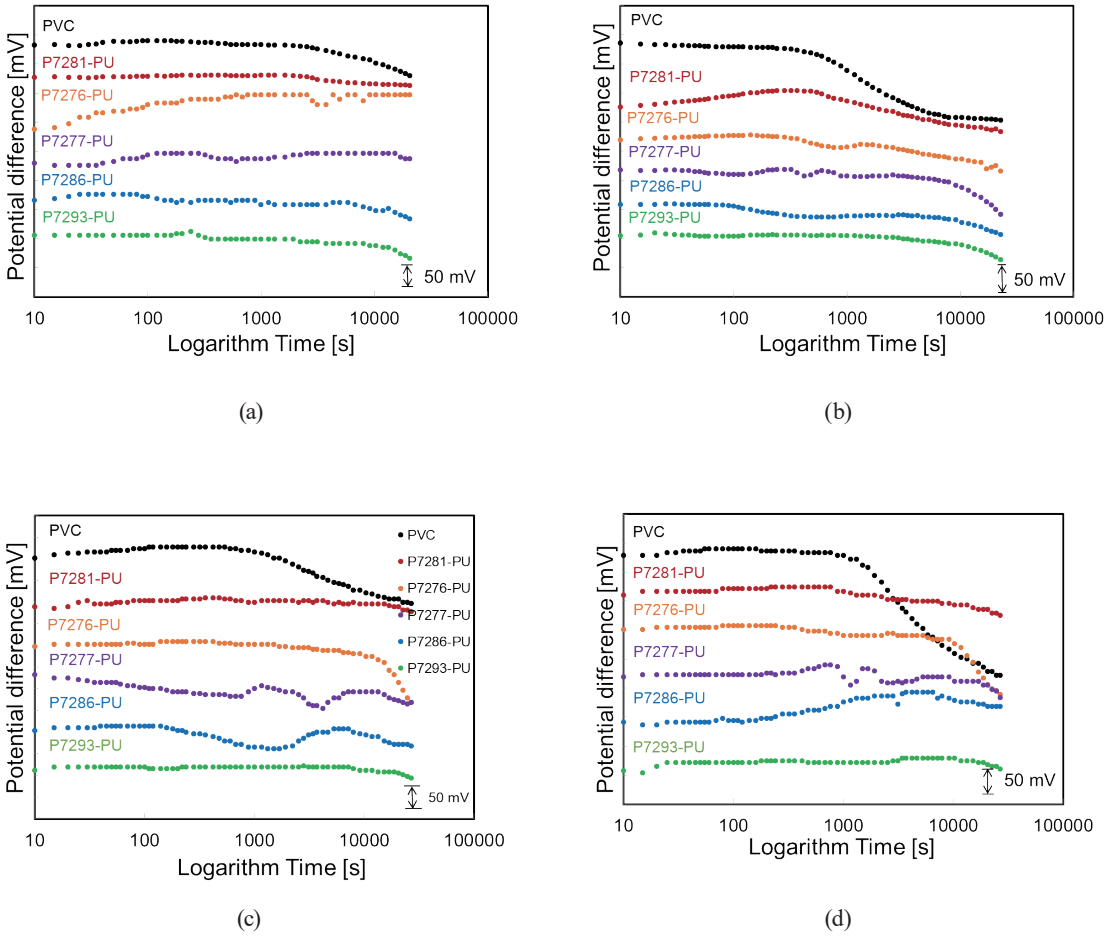

Fig. 6. (Color online) Drift characteristics of NO_3^--ISFETs: (a) in standard solution, (b) in standard solution with 0.5 wt% mucin, (c) in standard solution with 10 mM sodium bicarbonate, and (d) in artificial saliva.

Furthermore, the ISFETs based on P7293-PU showed a more stable response than the NO_3^--ISFETs based on P7281-PU in mucin solution.

3.3 Optical images of surface of ISFETs before and after drift measurement

We visually observed the surface conditions of the membranes with the NO_3-ISFETs based on the P72XX-PU series. The surfaces of the ISFETs using PVC and the P72XX-PU series were observed by optical microscopy before and after the drift measurement in the standard solution. All images are shown in Fig. 7.

The surfaces of the membranes including P7283-PU, P7287-PU, and P7290-PU [Figs. 7(e), 7(g), and 7(h), respectively] were considerably different from that of the membrane including PVC [Fig. 7(a)]. The NO_3^--ISFETs based on P7283-PU, P7287-PU, and P7290-PU did not show a reproducible response because the membrane was cracked. Furthermore, the surfaces of P7276-PU, P7277-PU, and P7286-PU, which showed a reproducible drift response, were slightly

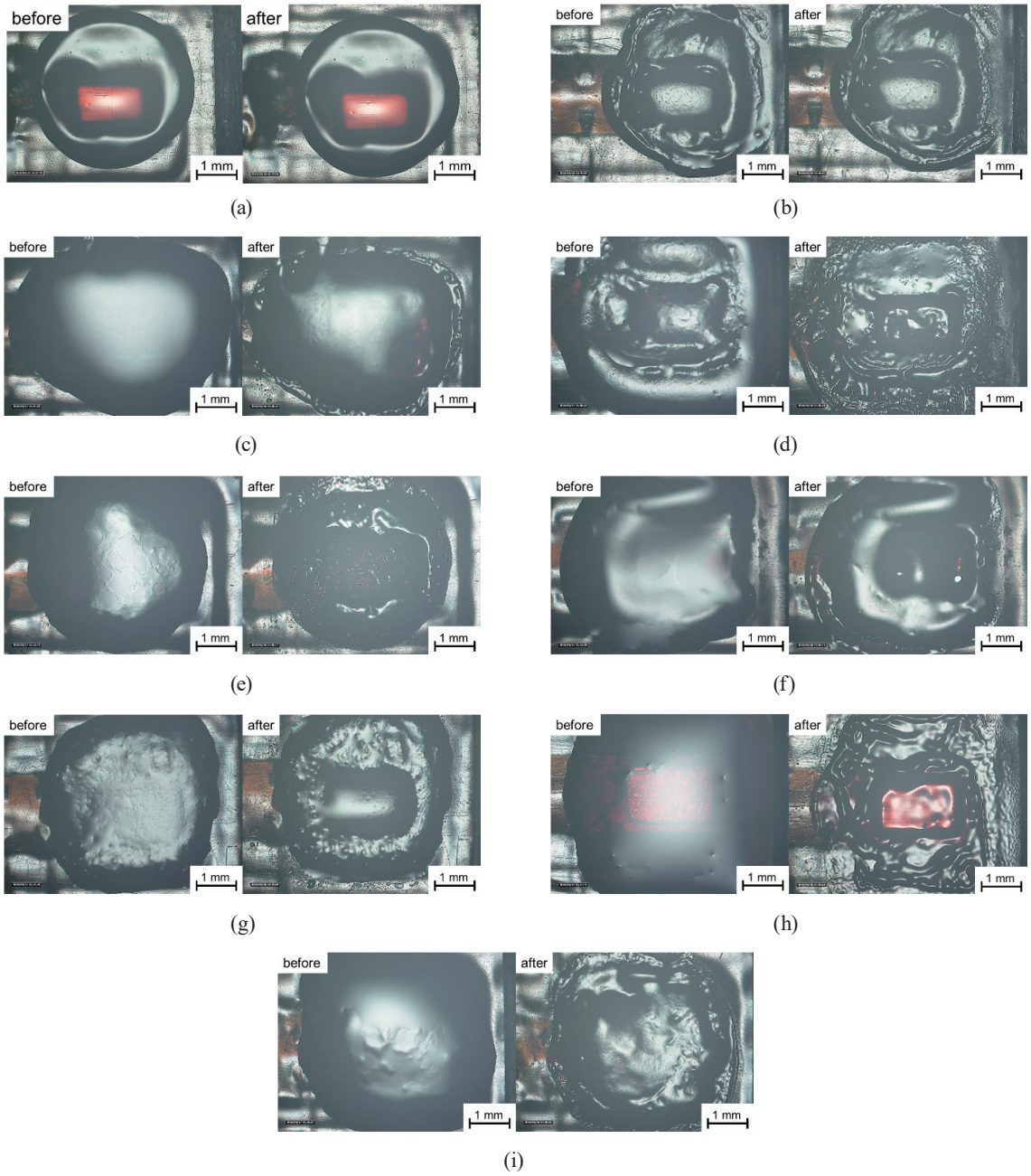

Fig. 7. (Color online) Images of surfaces of ISFETs based on PVC and P72XX-PU series before and after the drift measurement. (a) PVC, (b) P7281-PU, (c) P7276-PU, (d) P7277-PU, (e) P7283-PU, (f) P7286-PU, (g) P7287-PU, (h) P7290-PU, and (i) P7293-PU.

changed after the drift evaluation [see Figs. 7(c), 7(d), and 7(f), respectively]. The surface of P7293-PU was slightly changed, but the ISFETs based on P7293-PU showed the most stable drift response among the NO_3^--ISFETs (see Sect. 3.2). The surfaces of PVC and P7281-PU did not change [Figs. 7(a) and 7(b), respectively], and the ISFETs based on P7281-PU showed a stable drift response.

These results cannot be described in terms of our previous hypothesis[29] that H^+ or OH^- ions are captured in urethane bonds to prevent a pH change in the gate and the membrane interface of

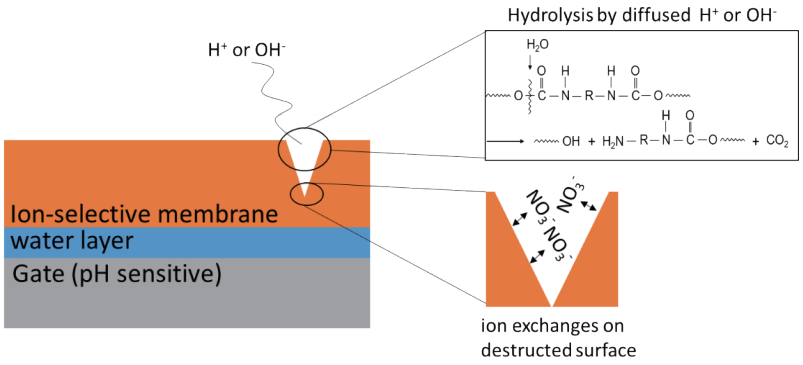

Fig. 8. (Color online) Hypothesis of urethane hydrolysis and ion sensing on cracked surface.

the ISFETs. In this study, the drift characteristics show a gradual fluctuation, probably depending on the pH change; however, the NO_3^--ISFETs based on P7276-PU, P7277-PU, and P7286-PU showed more rapid upward and downward drifts [see Figs. 6(c) and 6(d)].

We consider that the NO_3^--ISFETs based on the polyurethane matrix are controlled by the hydrolysis of the urethane bonds. The pH change in the aqueous layer between the gate and the ISM is prevented because the urethane bonds are hydrolyzed by the diffused H^+ or OH^-. However, the membrane structure is cracked by the urethane hydrolysis. Furthermore, we consider that the number of ion-trapping sites is increased by hydrolyzation. Therefore, the ratio of urethane bonds and the compatibility between the plasticizer and ISM are important. Since P7293-PU contains the most benzene ring structures, it leads to a high affinity for plasticizers, with its ion sensitivity maintained even after drift evaluation. P7281-PU has a high molecular weight with many urethane bonds to maintain its sensitivity. On the basis of the above discussion, we have improved our conventional hypothesis (Fig. 8): the hydrolysis of urethane bonds inhibits the diffusion of hydroxide ions, and the plasticizers contained on the ISM surface react with the nitrate. In the future, we hope to verify our hypothesis by analyzing the surface of the ISMs and observing its change over time.

4. Conclusions

We found that the ISFETs based on P7281-PU and P7293-PU are most effective for preventing drift, as shown in Figs. 6 and 7. Furthermore, mucin was less easily adsorbed on the surface of P7293-PU than on the surface of P7281-PU, because the hydrolysis of P7293-PU was faster than that of P7281-PU. In conclusion, we evaluated the hypothesis of the prevention effect of P7281-PU and other polyurethanes with the same backbone structure and different molecular weights. We found that the NO_3^--ISFETs based on P7293-PU showed less drift than those based on P7281-PU.

We consider that the drift and other sensor characteristics were controlled by the urethane hydrolysis. According to our hypothesis, the pH change in the aqueous layer between the gate and the ISM (one of the causes of the drift) is prevented because the urethane bonds are hydrolyzed by the diffused H^+ or OH^-.

In the future, we will evaluate the drift characteristics of NO_3^--ISFETs in real saliva samples. We will attempt to clarify the drift and the characteristics of the ISM. For this purpose, we will use the PVC-based ISM because of its simple structure compared with that of polyurethane at various pH values. Such work will contribute toward enabling the sensing of stress from human salivary ions.

Acknowledgments

This work was supported by AIST Open Innovation Arena Program, the JST COI Program "Design and manufacturing for the future based on individual needs in terms of healthy and enriched lifestyles" created by the Frontier Center for Organic System Innovations, and JSPS KAKENHI Grant Numbers JP19K21549 and JP19K05533.

References

1 C. Hammen: Annu. Rev. Clin. Psychol. **1** (2005) 293. https://doi.org/10.1146/annurev.clinpsy.1.102803.143938
2 K. S. Kendler and C. O. Gardner: Psychol. Med. **46** (2016) 1865. https://doi.org/10.1017/s0033291716000349
3 R. C. Kessler: Annu. Rev. Psychol. **48** (1997) 191. https://doi.org/10.1146/annurev.psych.48.1.191
4 E. J. Costello, D. S. Pine, C. Hammen, J. S. March, P. M Plotsky, M. A. Weissman, J. Biederman, H. H. Goldsmith, J. Kaufman, P. M. Lewinsohn, M. Hellander, K. Hoagwood, D. S. Koretz, C. A. Nelson, and J. F. Leckman: Biol. Psychiatry **52** (2002) 529. https://doi.org/10.1016/s0006-3223(02)01372-0
5 H. Nagai, Y. Narita, M. Ohtaki, K. Saito, and S. Wakida: Anal. Sci. **23** (2007) 975. https://doi.org/10.2116/analsci.23.975
6 B. Filip, J. Hans-Joachim, H. Volker, and O. Marcus: PLoS One **14 (**2019) e0221269. https://doi.org/10.1371/journal.pone.0221269
7 S. Andrew, M. Mika, L. Gordon, R. Ann, and H. Mark: Ann. Behav. Med. **50** (2016) 898. https://doi.org/10.1007/s12160-016-9817-5
8 S. Wakida: Proc. SPIE 11007, Adv. Environ. Chem. Biol. Sens. Technol. **XV** (2019) 1100702. https://doi.org/10.1117/12.2518851
9 E. Charmandari, C. Tsigos, and G. Chrousos: Annu. Rev. Physiol. **67** (2005) 259. https://doi.org/10.1146/annurev.physiol.67.040403.120816
10 K. O. Schwab, G. Heubel, and H. Bartels: Eur. J. Clin. Chem. Clin. Biochem. **30** (1992) 541. https://doi.org/10.1515/cclm.1992.30.10.0
11 S. Wakida, S. Osaki, T. Kintoki, K. Kitamura, Y. Murai, and T. Moriuchi-Kawakami: Proc. 17th Int. Meet. Chem. Sens. (Austria, 2018). https://doi.org/10.5162/IMCS2018/FE.6
12 E. F. Sato, T. Choudhury, T. Nishikawa, and M. Inoue: J. Clin. Biochem. Nutr. **42** (2008) 8. https://doi.org/10.3164/jcbn.2008002
13 I. Fleming and R. Busse: J. Mol. Cell. Cardiol **31** (1999) 5. https://doi.org/10.1006/jmcc.1998.0839
14 S. Wakida: Folia Pharmacol. Jpn. **141** (2013) 296. https://doi.org/10.1254/fpj.141.296
15 M. Toda, R. Den, M. Hasegawa-Ohira, and K. Morimoto: Complementary Ther. Med. **21** (2013) 29. https://doi.org/10.1016/j.ctim.2012.11.004
16 C. M. de Andrade, L. V. Galvao-Moreira, J. F. F. de Oliveira, M. R. Q. Bomfim, S. G. Monteiro, P. D. S. Figueiredo, and L. S. Branco-de-Almeida: J. Craniomandibular Sleep Pract. **7** (2019) 231. https://doi.org/10.1080/08869634.2019.1607445
17 K. Obayashi: Clin. Chim. Acta **425** (2013) 196. https://doi.org/10.1016/j.cca.2013.07.028
18 S. Cozma, C. Martu, C. M. Ghiciuc, F. R. Patacchioli, and L. C. D. Cozma: Rev. Chim. **69** (2018) 728. https://doi.org/10.37358/RC.18.3.6186
19 K. Kitamura, K. Murai, S. Wakida, T. Kintoki, and S. Osaki: Trans. Navig. **6** (2021) 1. https://doi.org/10.18949/jintransnavi.6.1_1
20 K. Kitamura, K. Murai, S. Wakida, S. Osaki, and T. Kintaki: 2021 World Automation Congr. (WAC) (2021). https://doi.org/10.23919/WAC50355.2021.9559481

21 E. J. Fogt, D. F. Untereker, M. S. Norenberg, and M. E. Meyerhoff: Anal. Chem. **57** (1985) 1995. https://doi.org/10.1021/ac00286a048
22 R. Patrick, D. W. Peter, P. Martin, S. H. Angela, E. M. Werner, F. R. Nico, and P. Erno: Anal. Chim. Acta **464** (2002) 79. https://doi.org/10.1016/S0003-2670(02)00475-0
23 N. Abramova, Y. Borisov, A. Bratov, P. Gavrilenko, C. Dominguez, V. Spiridonov, and E. Suglobova: Talanta **52** (2000) 533. https://doi.org/10.1016/s0039-9140(00)00408-2
24 J. Panu, F. Rantonen, and H. M. Jukka: Acta Odontol. Scand. **58** (2000) 160. https://doi.org/10.1080/000163500429154
25 J. Janata: Analyst **119** (1994) 2275. https://doi.org/10.1039/an9941902275
26 X. H. Li, E. M. J. Verpoorte, and D. J. Harrison: Anal. Chem. **60** (1988) 493. https://doi.org/10.1021/ac00156a025
27 T. Matsuo, H. Nakajima, T. Osa, and J. Anzai: Sens. Actuators **9** 1986) 115. https://doi.org/10.1016/0250-6874(86)80013-0
28 J. P. Veder, R. De Marco, G. Clarke, R. Chester, A. Nelson, K. Prince, E. Pretsch, and E. Bakkert: Anal. Chem. **80** (2008) 6731. https://doi.org/10.1021/ac800823f
29 S. Osaki, T. Kintoki, T. Moriuchi-Kawakami, K. Kitamura, and S. Wakida: Sensors **19** (2019) 2713. https://doi.org/10.3390/s19122713
30 S. Wakida, T. Okumura, Y. Shibutani, and H. Liu: Sens. Mater. **19** (2007) 235. https://sensors.myu-group.co.jp/index.php?vol=19&no=4&sub_no=0
31 Y. Ito: Sens. Actuators, B **66** (2000) 53. https://doi.org/10.1016/S0925-4005(99)00443-8
32 L. Zhang, J. Lu, and R. Maeda: Int. J. Adv. Networks Serv. **13** (2020) 108.
33 Y. Tanaka, N. Naruishi, H. Fukuya, J. Sakata, K. Saito, and S. Wakida: J. Chromatogr. A **1051** (2004) 193. https://doi.org/10.1016/j.chroma.2004.06.053

About the Authors

Shuto Osaki received his bachelor's degree in engineering from Osaka Institute of Technology, his M.Sc. degree in human development and environment from Kobe University, and his Ph.D. degree in engineering from Osaka University. He is a collaborative researcher in AIST–Osaka University Advanced Photonics and Biosensing Open Innovation Laboratory, National Institute of Advanced Industrial Science and Technology (AIST). He also has a Research Fellowship for Young Scientists from the Japan Society for the Promotion of Science (JSPS). His research interests are in the development of electrochemical biosensors, including ion-selective field-effect transistors (ISFETs) and amperometric sensors, and electrochemical impedance spectroscopy (EIS). He is also interested in the application of biosensors for human stress monitoring, diagnosis, and point-of-care testing.
(osaki@ap.eng.osaka-u.ac.jp)

Kenichi Kitamura received his Ph.D. degree in maritime science from Kobe University, Japan. He is an associate professor at the National Institute of Technology, Toba College and a visiting researcher of AIST–Osaka University Advanced Photonics and Biosensing Open Innovation Laboratory, National Institute of Advanced Industrial Science and Technology (AIST). (kitamura-k@toba-cmt.ac.jp)

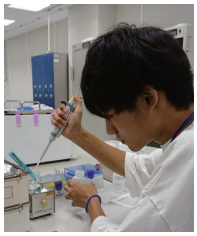

Takuya Kintoki received his master's degree from Osaka Institute of Technology, Japan. He is a research assistant of AIST–Osaka University Advanced Photonics and Biosensing Open Innovation Laboratory, National Institute of Advanced Industrial Science and Technology (AIST).

Takayo Moriuchi-Kawakami received her Ph.D. degree in engineering from Osaka University. She is presently a professor of Osaka Institute of Technology, Osaka, Japan. Her research interests are molecular recognition chemistry and chemical sensors.

Shin-ichi Wakida (M'87) received his Dr. Eng. degree from the University of Tokyo, Japan. He is presently vice-chief of the National Institute of Advanced Industrial Science and Technology (AIST)–Osaka University Advanced Photonics Biosensing Open Innovation Laboratory.